Journal of Magnetic Resonance **148,** 363–366 (2001)
doi:10.1006/jmre.2000.2250, available online at http://www.idealibrary.com on IDEAL®

Diffusion Measurements with the Aid of Nutation Spin Echoes Appearing after Two Inhomogeneous Radiofrequency Pulses in Inhomogeneous Magnetic Fields

Attila Scharfenecker, Ioan Ardelean,[1] and Rainer Kimmich

Sektion Kernresonanzspektroskopie, Universität Ulm, 89069 Ulm, Germany

E-mail: ioan.ardelean@physik.uni-ulm.de

Received July 21, 2000; revised October 26, 2000

Nutation echoes are generated by radiofrequency (RF) pulses with an inhomogeneous amplitude, $B_1 = B_1(r)$, in inhomogeneous magnetic fields, $B_0 = B_0(r)$. The two gradients of strengths G_1 and G_0, respectively, must be aligned in parallel for a maximum echo signal. After two RF pulses, two echoes appear at times $\tau_a = 2\tau_1 + \tau_2 + (G_1/G_0)\tau_1$ and $\tau_b = 2\tau_1 + \tau_2 + 2(G_1/G_0)\tau_1$, where τ_1 is the RF pulse duration and τ_2 the interpulse interval. It is shown that these echoes can favorably be employed for the determination of self-diffusion coefficients even in the poor experimental situation one often faces in low-resolution or low-field NMR. The signal intensity is comparable to that of ordinary Hahn echoes. Diffusion coefficients and spin–lattice relaxation times can be evaluated from the same experimental data set if both nutation echoes are recorded. Test experiments are in good agreement with literature data. Applications of the technique to "inside out" NMR, well logging NMR, surface coil NMR, toroid cavity NMR, etc., are suggested.

Key Words: **nutation echo; diffusion; radiofrequency gradients; localization.**

1. INTRODUCTION

NMR experiments for the determination of self-diffusion coefficients in liquids are usually based on gradients of the main magnetic field, B_0, ("laboratory frame techniques"). The gradients are applied either in pulsed or in steady form (*1, 2*). Alternatively, it has been suggested to employ gradients of the radiofrequency (RF) amplitude, B_1, (*3–6*) ("rotating-frame techniques"). In this paper a mixed gradient technique based on B_1 as well B_0 gradients is presented.

Recently, it was shown that in the presence of B_0 inhomogeneities one or two B_1 gradient pulses lead to one or two nutation echoes (*7–12*). Apart from these nutation echoes, "nonlinear" nutation echoes may appear in addition in high-field NMR (*9–11*). Here we restrict ourselves to the first two ("ordinary," i.e., linearly evolving) nutation echoes appearing after two B_1 gradient pulses (*11*). Note that the signal intensities of these echoes are comparable to those of conventional Hahn echoes.

The nutation echo technique for diffusion measurements to be proposed in this report can be implemented on any NMR setup. The imperfections of the B_1 and B_0 homogeneities that are often unavoidable in low-resolution and low-field NMR can readily be exploited for this purpose.

2. PULSE SEQUENCE

Figure 1 shows the pulse sequence of the new nutation echo diffusometry technique. The sequence consists of two RF pulses each of duration τ_1. The pulse spacing is τ_2. The pulses are subject to an RF amplitude gradient, G_1, and are applied in the presence of a steady gradient G_0 of the external magnetic flux density.

The first RF pulse splits the equilibrium magnetization into longitudinal and transverse components that are modulated along the B_1 gradient direction in the form of a helix. After this RF pulse, the transverse magnetization is assumed to be completely spoiled by B_0 gradients so that no interference with the subsequent nutation echoes is expected.

After a diffusion interval, τ_2, a second RF pulse again of width τ_1 converts the longitudinal magnetization that still exists at this time into modulated longitudinal and transverse components. The nutation echoes appear when the B_1 gradient "area" (strength times duration) is matched by the area of the subsequent (preferably spatially constant) B_0 gradient with respect to magnitude and direction (*10*). That is, a part of the longitudinal component is converted by the second RF pulse into a transverse component that then evolves in the presence of the B_0 gradient.

The coherences are refocused by the constant gradient in the form of two "nutation echoes" at times

$$\tau_a = 2\tau_1 + \tau_2 + \frac{G_1}{G_0}\tau_1 \quad \text{(echo a)} \qquad [1]$$

[1] On leave from Department of Physics, Technical University, 3400 Cluj-Napoca, Romania.

1090-7807/01 $35.00

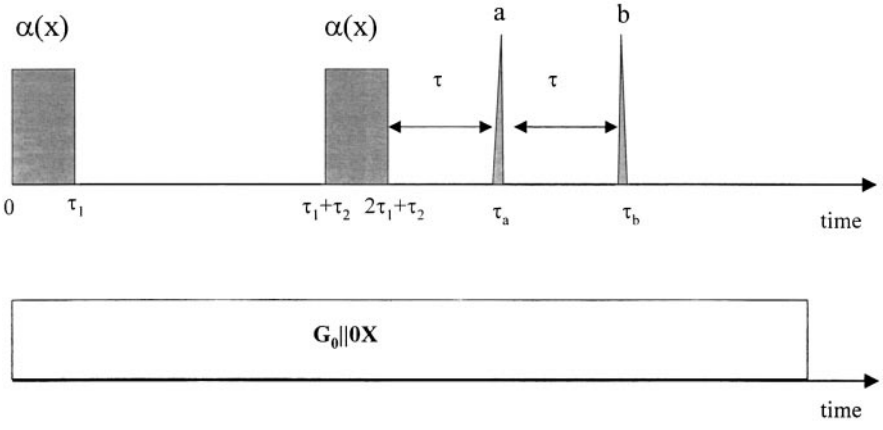

FIG. 1. Pulse sequence for the generation of two-pulse nutation echoes. The gradient of the RF pulse amplitude, G_1, and the gradient of the external magnetic field, G_0, must be aligned along the same direction (here assumed to be the X axis of the laboratory frame).

and

$$\tau_b = 2\tau_1 + \tau_2 + 2\,\frac{G_1}{G_0}\,\tau_1 \quad \text{(echo b)}. \tag{2}$$

The intervals between the second RF pulse and the two nutation echoes are given by

$$\tau = \frac{G_1}{G_0}\,\tau_1. \tag{3}$$

This is the gradient matching condition, where it is anticipated that the directions of both gradients coincide.

3. THEORY

The pulse sequence to be treated in the following is shown in Fig. 1 (*11*). The spin system under consideration consists of uncoupled spins $I = \frac{1}{2}$. The rotating-frame phase direction of the pulses is arbitrarily chosen to be x. The B_0 and B_1 gradients are both assumed along the X axis of the laboratory frame. Relaxation and diffusion during the RF pulses are neglected. The influence of the demagnetizing field on the considered nutation echoes (in contrast to multiple or nonlinear nutation echoes (*11*)) is minor and can therefore be neglected too (compare Refs. (*13, 14*)).

The spin-bearing particle is assumed to be at a position x at the time of the first RF pulse and at position x' after the interval τ_2. The displacement mechanism considered is unrestricted self-diffusion. The spin states generated by the first RF pulse can be represented by the reduced density operator deprived from all constant terms and factors as

$$\sigma(x,\,\tau_1) = I_y \sin[\alpha(x,\,\tau_1)] + I_z \cos[\alpha(x,\,\tau_1)], \tag{4}$$

where I_x and I_z are components of the spin vector operator. Since the B_1 gradient is to be constant within the sample, we have

$$\alpha(x,\,\tau_1) = \gamma G_1 x \tau_1, \tag{5}$$

where $G_1 = \partial B_1(x)/\partial x$. In case the transverse components are completely spoiled during τ_2, the density operator just before the second RF gradient pulse can be written as

$$\sigma(x,\,\tau_1 + \tau_2^-) = I_z[(1 - e^{-(\tau_2/T_1)}) + \cos\,\alpha(x,\,\tau_1)e^{-(\tau_2/T_1)}]. \tag{6}$$

In this expression, longitudinal and transverse relaxation characterized by the relaxation times T_1 and T_2, respectively, have phenomenologically been accounted for (*6, 15*). Previously we have shown (*11*) that the coherences corresponding to the two terms in the density operator are refocused by the second RF pulse in the form of the two nutation echoes provided that the main magnetic field is subject to a gradient in the same direction as the B_1 gradient. The unmodulated term provides the echo "*a*" at τ_a given by Eq. [1], whereas the modulated one leads to an echo signal "*b*" at τ_b according to Eq. [2].

Since the spin under consideration diffuses to a position x' during τ_2, the tip angle generated by the second RF pulse will consequently be a function of this position. The density operator immediately after the second RF pulse reads

$$\begin{aligned}\sigma(x,\,x',\,\tau_1 + \tau_2^+) &= [I_z \cos\,\alpha(x',\,\tau_1) + I_y \sin\,\alpha(x',\,\tau_1)] \\ &\quad \times [(1 - e^{-(\tau_2/T_1)}) + \cos\,\alpha(x,\,\tau_1)e^{-(\tau_2/T_1)}].\end{aligned} \tag{7}$$

Unrestricted normal diffusion characterized by the self-diffusion coefficient D is described by a Gaussian displacement propagator,

$$\mathcal{P}(x - x',\ \tau_2) = \frac{1}{\sqrt{4\pi D\tau_2}}\, e^{-(x-x')^2/(4D\tau_2)}. \qquad [8]$$

As a consequence, the differences in the nutation angles produced by the first and the second RF pulse are also distributed according to a Gaussian. Expressing the initial position, x, as a function of the final position, x', the density operator, Eq. [7], can be rewritten as

$$\begin{aligned}\sigma(x, x',\ \tau_1 + \tau_2^+) &= [I_z \cos\,\alpha(x',\ \tau_1) + I_y \sin\,\alpha(x',\ \tau_1)] \\ &\times [(1 - e^{-(\tau_2/T_1)}) + \cos\,\alpha(x',\ \tau_1) e^{-(\tau_2/T_1)} \langle e^{i\gamma G_1 (x-x')\tau_1}\rangle].\end{aligned} \qquad [9]$$

The attenuation factor $\langle e^{i\gamma G_1 (x-x')\tau_1}\rangle$ is formed as an ensemble average over all spins in the sample. It accounts for the fact that the local nutation angles of the first and second RF pulses deviate from each other owing to the displacements of the spin-bearing particles in the interval between the pulses. Using the probability density Eq. [8], the attenuation factor is found to be

$$\langle e^{i\gamma G_1 (x-x')\tau_1}\rangle = e^{-D(\gamma G_1)^2 \tau_1^2 \tau_2}. \qquad [10]$$

After the second RF pulse, the coherences evolve in the presence of the constant gradient G_0. Forming the average of the density operator over all x' positions in the sample then leads to an expression predicting the formation of nutation echoes (*11*). The first echo at the time τ_a (Eq. [1]) originates from the unmodulated term in Eq. [6]. The amplitude is

$$A_a(\tau_a) = \frac{M_0}{2}\,(1 - e^{-(\tau_2/T_1)}) e^{-(\tau/T_2)}. \qquad [11]$$

This echo is based on the fraction of the longitudinal magnetization that is reestablished by spin–lattice relaxation during τ_2. It thus has the character of an ordinary nutation echo (*10*) weighted by the spin–lattice relaxation term. The underlying coherences are exclusively excited by the second RF pulse.

The modulated term in Eq. [6] leads to the second echo at the time τ_b (Eq. [2]) with the amplitude

$$A_b(\tau_b) = \frac{M_0}{4}\, e^{-(\tau_2/T_1)} e^{-(2\tau/T_2)} e^{-D(\gamma G_1)^2 \tau_1^2 \tau_2}. \qquad [12]$$

The coherences responsible for this echo can be traced back as such to the first RF pulse.

Note that only the second echo is attenuated by diffusion, whereas the first one is solely affected by relaxation (provided that diffusion in the τ interval can be neglected). That is, keeping τ constant in an experiment, one can determine the spin–lattice relaxation time T_1 from the variation of the first echo with τ_2 and, based on this information, the diffusion coefficient D from the attenutation of the second echo. Both quantities can thus be determined from a single experimental data set. The diffusion attenuation of the second nutation echo (see Eq. [12]) has the same characteristics as that known from stimulated-echo experiments (*2*).

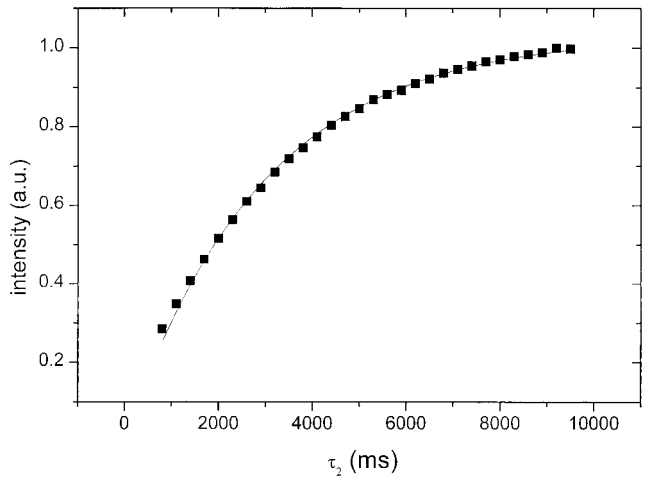

FIG. 2. Amplitude of the first nutation echo "*a*" for cyclohexane as a function of the interval τ_2. The solid line represents Eq. [11] fitted to the experimental data. A total number of eight scans with a repetition time of 30 s were accumulated.

4. RESULTS

Test experiments were carried out with cyclohexane at 298 K. The sample tubes were 3 mm long and 4 mm thick. The measurements were performed with a Bruker DPX400 spectrometer operating at 400-MHz proton resonance. The B_1 gradients for the pulse sequence in Fig. 1 were produced with a four-turn conic transmitter and receiver coil as described in Ref. (*11*). The pulse length was adjusted to $\tau_1 = 326\ \mu$s, so that both relaxation and diffusion during the pulses can safely be neglected. The B_1 gradient turned out to be fairly constant in the sample and was calibrated using the known diffusion coefficient of distilled water ($D = 2.3 \cdot 10^{-9}$ m^{2}s).

The main magnetic field was subject to a steady gradient $G_0 \cong 10$ mT/m by intentionally misadjusting the shim currents. This gradient simultaneously serves spoiling of undesired coherences after the first RF pulse. The nutation echo signals were acquired at intervals $\tau = 10$ ms and $2\tau = 20$ ms after the second RF pulse. The echo intensity was evaluated by integrating the signal over a small interval in order to avoid errors due to gradient variation across the sample.

Figure 2 shows the amplitude of the first nutation echo as a function of the diffusion interval τ_2 varied between 0.8 and 10 s. Using Eq. [11], the value of the longitudinal relaxation

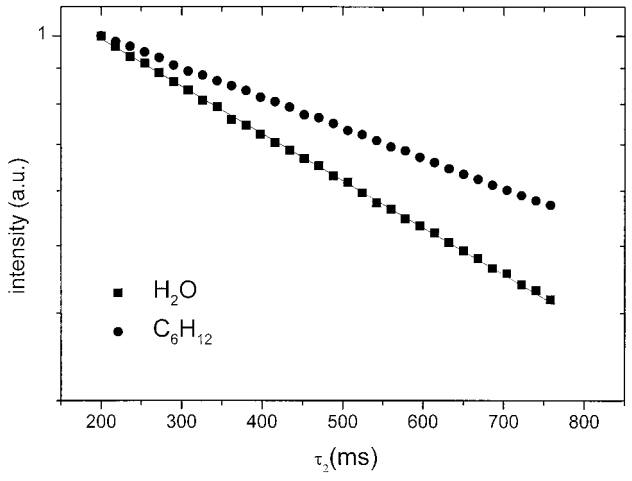

FIG. 3. Amplitude of the second nutation echo "*b*" for water and cyclohexane as a function of the interval τ_2. The solid line represents Eq. [12] fitted to the cyclohexane data. A total number of eight scans with a repetition time of 30 s were accumulated.

time for cyclohexane was determined as $T_1 = 2.94$ s. This value was then anticipated in the fitting procedure for the diffusion coefficient according to Eq. [12]. Figure 3 shows the decay of the nutation echo amplitude as a function of the evolution interval between 200 and 800 ms for water and cyclohexane. From the water data, the B_1 gradient was determined as $G_1 = 299$ mT/m. Based on this value, the diffusion coefficient of cyclohexane was found to be $D = 1.49 \cdot 10^{-9}$ m^2/s, in good agreement with previously reported results (*16*).

5. CONCLUSIONS

It has been shown that two-pulse nutation echoes are suitable for diffusion measurements. The pulse sequence is particularly simple and easy to implement. It consists of only two RF pulses with B_1 gradients in the presence of a steady B_0 gradient. Both gradient directions must be parallel, and the gradient "areas" must match each other. Note that no extra RF receiver coil is needed as in other B_1 gradient-based methods (*6*).

The geometry of the RF coil employed in the test experiments was designed in a way to produce a constant B_1 gradient. Other geometries such as toroid cavities (*17*) provide stronger but spatially inhomogeneous RF field gradients. That is, a pronounced localization effect is expected in this case owing to the matching condition Eq. [3] (with respect to gradient magnitudes as well as directions) (*12*). In this way, localized diffusion and relaxation measurements become feasible. Studies of this sort may be of interest in context with applications of the NMR MOUSE (*18*) or well logging NMR devices (*19*).

An advantage of the two-pulse nutation echo pulse sequences is that the diffusion coefficient as well as the longitudinal relaxation time can be extracted from the same experimental data set. The method can moreover easily be modified for flow phase-encoding experiments. A further option is to use pulsed B_0 gradients instead of the steady ones assumed here. In this case, spectral information can be extracted by Fourier transforming the echo induction signals.

ACKNOWLEDGMENTS

This work has been supported by the Deutsche Forschungsgemeinschaft and the Alexander von Humboldt Stiftung.

REFERENCES

1. J. Kärger, H. Pfeifer, and W. Heink, *Adv. Magn. Reson.* **12,** 1–89 (1988).
2. R. Kimmich, "NMR Tomography, Diffusometry, Relaxometry," Springer-Verlag, Berlin, 1997.
3. D. Canet, B. Diter, A. Belmajdoub, J. Brondeau, J. C. Boubel, and K. Elbayed, *J. Magn. Reson.* **81,** 1–12 (1989).
4. R. Dupeyre, P. H. Devoulon, D. Bourgeois, and M. Decorps, *J. Magn. Reson.* **95,** 589–596 (1991).
5. R. Kimmich, B. Simon, and H. Köstler, *J. Magn. Reson. A* **112,** 7–12 (1995).
6. D. Canet, *Prog. NMR Spectrosc.* **30,** 101–135 (1997).
7. A. L. Bloom, *Phys. Rev.* **98,** 1105–1111 (1955).
8. R. Kaiser, *J. Magn. Reson.* **42,** 103–109 (1981).
9. A. Jerschow, *Chem. Phys. Lett.* **296,** 466–470 (1998).
10. R. Kimmich, I. Ardelean, Y.-Y. Lin, S. Ahn, and W. S. Warren, *J. Chem. Phys.* **111,** 6501–6509 (1999).
11. I. Ardelean, A. Scharfenecker, and R. Kimmich, *J. Magn. Reson.* **144,** 45–52 (2000).
12. I. Ardelean, R. Kimmich, and A. Klemm, *J. Magn. Reson.* **146,** 43–48 (2000).
13. I. Ardelean and R. Kimmich, *Chem. Phys. Lett.* **320,** 81–86 (2000).
14. G. Deville, M. Bernier, and J. M. Delrieux, *Phys. Rev. B* **19,** 5666–5688 (1979).
15. D. E. Demco, A. Johansson, and J. Tegenfeldt, *J. Magn. Reson. A* **110,** 183–193 (1994).
16. M. Holz and H. Weingärtner, *J. Magn. Reson.* **92,** 115–125 (1991).
17. K. Woelk, J. W. Rathke, and R. J. Klinger, *J. Magn. Reson. A* **105,** 113–116 (1993).
18. B. Blümich, P. Blümler, G. Eidmann, A. Guthausen, R. Haken, U. Schmitz, K. Saito, and G. Zimmer, *Magn. Reson. Imaging* **16,** 479–484 (1998).
19. R. L. Kleinberg, and C. Flaum, Review: NMR detection and characterization of hydrocarbons in subsurface Earth formations, *in* (P. Blümler, B. Blümich, R. Botto, and E. Fukushima, Eds.), "Spatially Resolved Magnetic Resonance," pp. 555–573, Wiley-VCH, Weinheim, 1998.